Title of the CMSC Technical Paper: Proposed E57.02 Range Measurement Performance Standard for Medium Range 3D Imaging Systems

Authors Names/Companies: David K. MacKinnon/National Research Council Canada, Luc Cournoyer/National Research Council Canada, Kamel Saidi/National Institute of Standards and Technology, Geraldine Cheok/National Institute of Standards and Technology, Robert Bridges/FARO Technologies, Darin Ingimarson/QinetiQ North America

Contact information for submitting Author: David MacKinnon, Ph.D., P.Eng.
Measurement Science and Standards Portfolio, Emerging Technologies Division, National Research Council of Canada
1200 Montréal Road, Ottawa, ON, K1A 0R6, Canada
Phone Number: (613)993-0114

Email: david.mackinnon@nrc-cnrc.gc.ca

Word Count: 3994

Number of Images Submitted: 8

Proposed E57.02 Test Method to Evaluate the Range Measurement Performance of 3D Imaging Systems in the Medium Range

David MacKinnon[1] and Luc Cournoyer
National Research Council of Canada, Measurement Science and Standards
Ottawa, Ontario, Canada, K1A 0R6

and

Kamel Saidi and Geraldine Cheok
National Institute of Standards and Technology, Engineering Laboratory
Gaithersburg, Maryland, USA, 20899-8611

and

Robert Bridges
FARO Technologies
Kennett Square, Pennsylvania, USA, 19348

and

Darin Ingimarson
QinetiQ North America, Technology Solutions Group
Pittsburgh, Pennsylvania, USA, 15238

Abstract

We present the proposed standard ASTM E57.02 "Test Method to Evaluate the Range Measurement Performance of 3D Imaging Systems in the Medium Range" (Work Item ASTM WK12373). The stated purpose of the standard is to provide metrics and procedures to evaluate the range measurement performance of medium-range (2 m to 150 m working distance) non-contact, three dimensional (3D) imaging systems. We provide a summary of the document to date, the proposed test methods, and the current status of the proposed standard. As an example, we also present preliminary results of experiments performed at the National Research Council Canada (NRCC).

Keywords: ASTM, E57, non-contact 3D imaging system, standard, system performance, range measurement system, range error, medium-range systems

1   Introduction

The ASTM working group WK12373[2] has been developing a method for evaluating the range measurement performance of medium-range (2 m to 150 m working distance) scanning laser-based 3D imaging systems. This working group is part of the ASTM E57 committee that develops standards for 3D imaging systems. In this paper we explain the test protocol and analytical procedure, and present an example to show how the standard would be used. We then draw some conclusions before briefly describing future work by the ASTM E57.02 task group.

---

[1] Primary author: david.mackinnon@nrc-cnrc.gc.ca
[2] http://www.astm.org/DATABASE.CART/WORKITEMS/WK12373.htm

To facilitate discussion we have adopted a formal nomenclature for variables. Scalar variables are indicated by lower-cased italicized characters (e.g., d), vectors by lower-cased characters that are both italicized and bold-faced (e.g., $\boldsymbol{p}$). Matrices are presented using upper-cased letters that have been bold-faced (e.g., $\mathbf{M}$). Best-fit models generated from data sets are indicated as matrices with a hat (e.g., $\hat{\mathbf{M}}$) to indicate that this is a data set derived from a fitting process and will use the same letter as the data set from which it was derived.
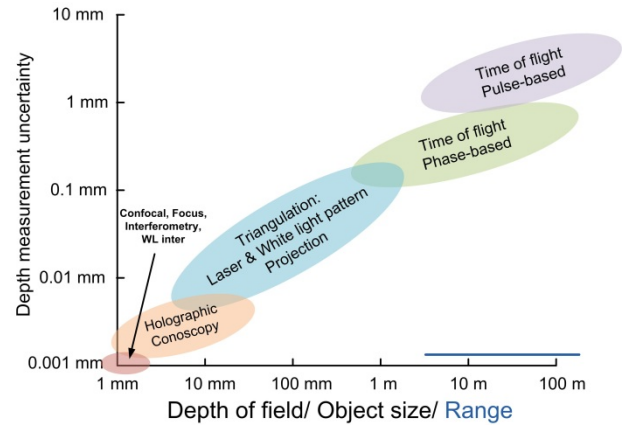

Figure 1: Expected depth (range) measurement uncertainty level as a function of depth-of-field/object size for different non-contact 3D imaging methods [1].

2 Background

In this section we provide an overview of the proposed standard. We also briefly introduce the reader to artifact-based evaluation of 3D imaging systems, a key area of research conducted by the 3D metrology team at National Research Council Canada (NRCC).

2.1 History

In 2006, the ASTM E57 committee was formed to develop standards to evaluate 3D imaging systems [2, 7]. The development of the committee was driven by the needs of users and product developers to assess the fitness-for-purpose of a given system, to compare instruments in a fair manner, and to evaluate instrument warranty issues through the assessment of compliance or non-compliance to manufacturer-claimed specifications [7]. The E57.02 subcommittee on test methods initially began evaluating range error of medium-range 3D imaging systems based on distance, target reflectivity, angle of incidence, and azimuth angle using a combination of spherical and planar target structures [2, 3]. Figure 1 shows how different 3D imaging system technologies compare with regard to expected depth (range) measurement uncertainty under rated conditions. Measurement uncertainty is the dispersion calculated from multiple error measurements so represents the random component of a measurement error model. For time-of-flight (TOF) 3D imaging systems, object size can be considered analogous to range. A maximum range of 150 m for medium range systems was selected to represent the typical size of projects employing pulsed- and phase-based TOF 3D imaging systems (e.g., building and bridges) [3].

Based on early experiments by the National Institute of Standards and Technology (NIST) [3, 10], FARO Technologies [6], and the NRCC [7], it was decided that a planar target would be used for range error analysis [2]. Spheres eliminated the need to orient the target, but producing spheres 300 mm or more in diameter for testing the upper-end of the 150 m range was expected to be cost-prohibitive [3]. Moreover, planar surfaces were shown to generate less noise than spherical surfaces [8]. The use of real-world materials was also abandoned as being impractical given the large number of possible materials. Spectralon[3], an industry-standard material for testing optical systems, was also considered but was

---

[3] Disclaimer: Although certain commercial products are mentioned, the inclusion of such information should in no way be construed as indicating that such products are endorsed by the authors or the institutions they represent, or that they are necessarily the best equipment for the purposes described.

discarded because of its cost and the fact that lasers operating in the wavelengths common to medium-range 3D imaging systems (500 nm to 1600 nm) penetrated the material by as much as 3 mm [2, 4]. Further experimentation focused on surfaces made of aluminum that had been vapor- or sand-blasted to provide a diffusely-reflecting surface [2].

Figure 2: Graphical representation of the target plates with respect to the origin of the instrument under test.

2.2 Range Error Standard

The purpose of this standard is to provide a structure within which to evaluate the range measurement performance of medium-range 3D imaging systems. This standard can be used to compare the performance among similar systems, to assess the observed versus claimed range measurement performance of a system, or to simply characterize the range measurement performance of a system. If used to assess warranty claims, then the evaluation described in this standard should be performed in accordance with manufacturer-supplied specifications and under rated conditions.

Metrological traceability is an informational path through measurement results and not through instruments [5] so, for a medium-range 3D imaging system, traceability stops at the reference instrument (RI). The RI is typically either a laser tracker or total station that uses a spherically-mounted retro-reflector (SMR) target, which is a well-calibrated and cooperative target [6]. The target surfaces used in the proposed E57 standard are non-cooperative, so it is not currently feasible to attain traceability from the RI to the instrument under test (IUT) except on a case-by-case basis [5].

The test method consists of comparing the distance measured between the geometric centers of two target plates by the IUT to the plate-to-plate distance measured by a RI. This means that the distance being evaluated is the relative distance (distance between two points), not the absolute distance from the origin/center of the IUT to a point on a target. Because the origin of many 3D imaging systems is typically unknown or not readily measurable, the task group decided to use relative distance so that the test method would not be restricted to certain classes of 3D imaging system.

Ranging error has two primary components: a constant origin offset, or R0, error and an incremental distance error [6]. As illustrated in Figure 2, the target plates are each oriented such that the line (Line A) passing through the geometric centers C_{near} and C_{far} of the target plates, and as much as possible, also passes through the origin O, and along the line-of-sight, of the IUT. The target plates are oriented so that the normal vectors of the front surfaces (faces) of the target plates are both aligned along Line A and directed toward O. In this configuration the constant R0 error is effectively cancelled out so the distance error component of the ranging error dominates the resulting range error value. See [6] for a more detailed description of the geometric errors associated with this test.

The manufacturer specifies C_{near}, which is the distance at which the IUT yields the smallest range error. The rationale for having the manufacturer specify this distance is to minimize the calculated range error. If the manufacturer does not specify this distance, then the user may choose any distance for C_{near}. C_{far} is selected by the user but must be within the rated conditions of the IUT.

2.3 Artifact-based Evaluation

In an artifact-based system evaluation, an artifact is used to connect the results obtained from the RI to the results obtained from the IUT. This process requires that the artifact, in this case a target plate, be selected such that it minimally affects the characteristic being evaluated. For range error evaluation, it is
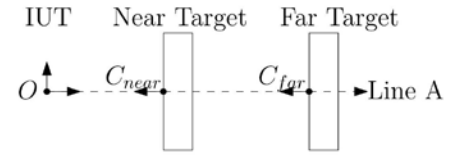
Figure 3: Example of a typical target plate. (a) Mounted on a target stand. (b) Mounted on a rail system.

important to minimize the influence of the target plate on the ability of the RI and IUT to fit a plane to the front surface (face) of that target plate. The standard requires that the target plate meet the manufacturer's optical and mechanical specifications, if any were provided. Moreover, the flatness of the target-plate face must not exceed 20% of the range error of the IUT. As a result, the performance of the IUT should be, for all intents and purposes, relative only to the performance of the RI.

An example of an acceptable artifact mentioned in the standard is an aluminum plate with a vapor-blasted finish (an example of which is shown in Figure 3); however, the user is free to choose any material, such as ceramic or steel, that meets the target-plate specifications. The user is required to document the flatness, reflectance factor, and diffuse reflectance factor of the target-plate face. The latter two values represent the amount of optical energy reflected by the target-plate face, with diffuse reflectance factor being the reflectance factor after the specular reflectance component has been removed [9].

3   Test Procedure

In this section we explain the procedure for performing a range error test. The test procedure involves two target plates, but can be adapted to more than two target plates. The test generates two characteristic values: Range error E_{range} and root-mean-squared (RMS) dispersion limit L_{RMS}. These characteristic values, and how they can be used to assess a medium-range 3D imaging system, are discussed in this section.

3.1   Setup

The test setup involves placing two target plates along Line A as illustrated in Figure 2 such that Line A passes through C_{near}, C_{far}, and O, and the normal vectors of the target-plate faces are aligned along Line A and directed toward O. The arrangement can also be generated using a single target plate moved to C_{near} and C_{far} as required. The RI is used to assist in achieving this setup as closely as is practically achievable. The setup is reasonably error-tolerant provided sufficient care is taken in positioning the target plates with respect to the IUT. The standard provides a more detailed example of how one can achieve a reasonably-accurate target-plate setup.

The target plate must be rigidly mounted so that it does not move during both RI and IUT measurement steps. The standard provides an example of target plate, RI, and IUT mounting assemblies that can ensure instrument and target-plate stability while performing data collection.

3.2 Data Collection

Data collection takes place in two steps: target-plate separation measurement by the RI and target-plate separation measurement by the IUT. The standard specifies that the expanded uncertainty of the range portion of the RI must be one quarter or less of the maximum permissible error (MPE) of the IUT. The RI is used to obtain a reference distance between the geometric centers of the two target-plate faces, d_{ref}, and the IUT is used to obtain a measured distance between the geometric centers of the two target-plate faces, d_{meas}. The test procedure involves the steps described in the sections 3.2.1 through 3.2.3 below. For purposes of illustration, the steps are described using a laser tracker as the RI, and the target plate farthest from the IUT is measured first.

3.2.1   RI measurement of the far target plate face

A SMR is used to obtain position measurements at widely-distributed points on the target-plate face so that a plane can be accurately fit to the measurement data obtained using the RI. Additional position measurements are obtained for all four sides bounding the target-plate face so that the bounds of the target-plate face can be established. The geometric center of the target-plate face, $\hat{\boldsymbol{p}}_{far,RI} = [\hat{x}_{far,RI} \quad \hat{y}_{far,RI} \quad \hat{z}_{far,RI}]^T$, in the RI coordinate system is calculated to be the centroid of the volume contained within the bounds of the target-plate face. The procedure used to generate the planes associated with the RI measurement results and how to use those planes to obtain $\hat{\boldsymbol{p}}_{far,RI}$ is described in Section 4.2.

3.2.2   IUT measurement of the far target-plate face

The IUT is used to capture a surface map of the target-plate face. The target-plate face must be large enough so that at least 100 IUT measurement results, relatively evenly distributed across the entire target-plate face, remain after an exclusion region around the edge of the target-plate face has been removed. Figure 4(a) shows an example of acceptable and unacceptable measurement distributions. An acceptable measurement distribution consists of measurements that are relatively evenly distributed across the entire target plate face and extend beyond the edges of the target plate face. Figure 4(b) illustrates the user-selected and exclusion regions to be applied to the surface map obtained by the IUT. If possible, no filtering or automatic point removal should be applied to the data collected by the IUT.

The first task is to obtain a best-fit plane $\widehat{W}_{far}$ to approximate the position, orientation, and bounds of the plane corresponding to the target plate face. Let $\mathbf{P}_{far}$ be the set of measured points obtained by the IUT, excluding all measurements the operator can clearly attribute to surfaces other than the target-plate face. A subset $\mathbf{S}_{far} \subseteq \mathbf{P}_{far}$ is selected by eliminating from $\mathbf{P}_{far}$ all points in the exclusion region so that $\mathbf{S}_{far}$ only represents points in the user-selected region, indicated by the grey-shaded region in Figure 4(b). The standard specifies that $\mathbf{S}_{far}$ should:

1. cover at least 50 % of the target-plate face area;
2. avoid the region affected by the edges of the target-plate face, referred to as the exclusion region. In Figure 4(b), the exclusion region is illustrated as a grey-hatched region bounded on the inside with dashed lines and the outside by the target plate face edge. The user-selected region (shown in grey) must be completely within the boundary indicated by dashed lines, referred to in Figure 4(b) as the bounds on the selection region;
3. contain at least 100 measured points, relatively evenly distributed across the entire target-plate face;
4. have a width w_{in} and height h_{in} no less than 10 times the beam diameter at that distance from the IUT.
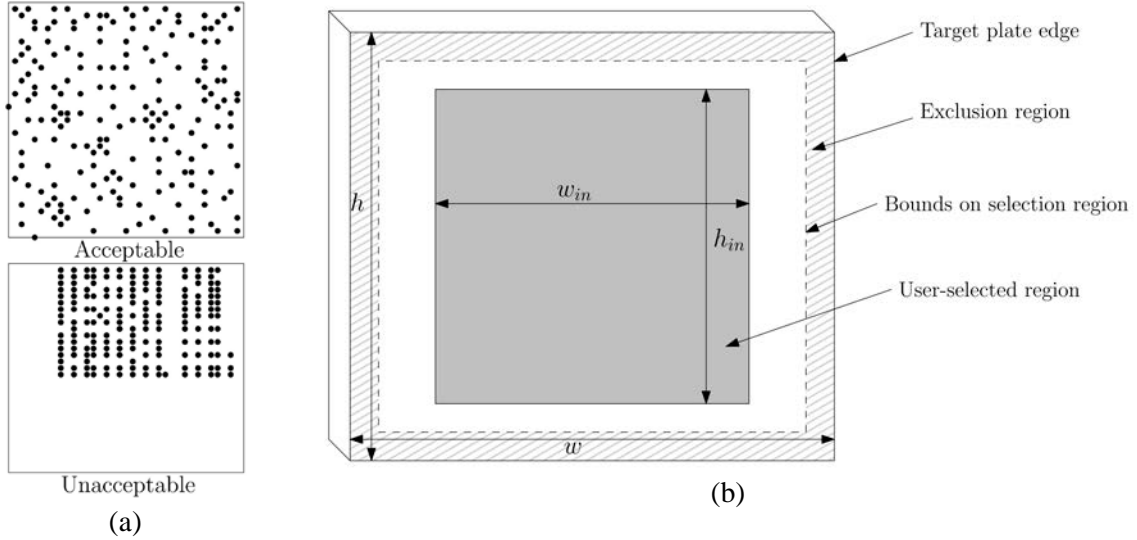
Figure 4: (a) Examples of acceptable and unacceptable measurement distribution across the target-plate face. (b) User-selected and exclusion regions for IUT measurement data.

A plane $\hat{\mathbf{S}}_{far}$ is then fitted to $\mathbf{S}_{far}$ using the method of least-squares regression, what is referred to as Orthogonal Least-squares Regression (OLS). In OLS regression, the residual is the amount by which each data point deviates from the model (in this case a plane) being fit to that data. Each residual is calculated from the orthogonal (shortest in Cartesian space) distance between each data point and the plane [11]. The standard deviation of the residuals s_{far} is also calculated at this time.

The second task is to estimate the geometric center of the target plate face from the IUT measurement results. This involves extending the edges of $\hat{\mathbf{S}}_{far}$ to generate a plane $\widehat{\mathbf{W}}_{far}$ that is bounded by the edges of the target plate face. We generate a bounding box for $\widehat{\mathbf{W}}_{far}$ that encompasses all points associated with the target plate face while, as much as possible, eliminating points affected by the edges of the target plate face. The points are then projected onto $\widehat{\mathbf{W}}_{far}$ and the smallest 2D bounding box that contains all the projected points is generated on $\widehat{\mathbf{W}}_{far}$. The geometric center of the bounding box is then an approximation of the geometric center of the target plate face.

To do this, we first remove from $\mathbf{P}_{far}$ any measured points more than $2s_{far}$ from $\hat{\mathbf{S}}_{far}$, measured orthogonal to $\hat{\mathbf{S}}_{far}$, to generate $\mathbf{W}_{far} \subseteq \mathbf{P}_{far}$. We then extend the edges of $\hat{\mathbf{S}}_{far}$ until it is bounded by the smallest possible 2D rectangular box that contains the orthogonal projection of every point in $\mathbf{W}_{far}$, calling this extended plane $\widehat{\mathbf{W}}_{far}$ The geometric center of $\widehat{\mathbf{W}}_{far}$ is then calculated to be the centroid of the bounds of the smallest bounding box that completely encompasses $\widehat{\mathbf{W}}_{far}$. The centroid, $\widehat{\boldsymbol{p}}_{far,IUT} = [\hat{x}_{far,IUT} \quad \hat{y}_{far.IUT} \quad \hat{z}_{far,IUT}]^T$, is an estimate of the geometric center of the target plate face in the IUT coordinate system. At this time, the RMS of the orthogonal distances from every point in $\mathbf{W}_{far}$ and the plane is calculated to be RMS_{far}.

3.2.3   RI and IUT measurement of the near target-plate face

The procedures described in Section 3.2.1 are used to generate the geometric center of the target-plate face at C_{near}, $\widehat{\boldsymbol{p}}_{near} = [\hat{x}_{near,RI} \quad \hat{y}_{near,RI} \quad \hat{z}_{near,RI}]^T$, in the RI coordinate system. The procedures

described in Section 3.2.2 are then used to generate the geometric center of the target-plate face, $\hat{\pmb{p}}_{near} = [\hat{x}_{near,IUT} \quad \hat{y}_{near,IUT} \quad \hat{z}_{near,IUT}]^T$, in the IUT coordinate system, as well as RMS_{near}.

3.3 Analysis of Results

The results obtained in Section 3.2 are used to calculate the range error, E_{range}, and the RMS dispersion limit, L_{RMS}. These results can be compared to manufacturer-provided specifications to determine whether the system is operating within the manufacturer's specified maximum permissible error for range, MPE_{range}, and the maximum permissible limit for RMS dispersion ,MPL_{RMS}.

Range error E_{range} is calculated as

$$E_{range} = d_{IUT} - d_{RI} \tag{1}$$

where

$$d_{IUT} = \sqrt{\left(\hat{x}_{far,IUT} - \hat{x}_{near,IUT}\right)^2 + \left(\hat{y}_{far,IUT} - \hat{y}_{near,IUT}\right)^2 + \left(\hat{z}_{far,IUT} - \hat{z}_{near,IUT}\right)^2} \tag{2}$$

and

$$d_{RI} = \sqrt{\left(\hat{x}_{far,RI} - \hat{x}_{near,RI}\right)^2 + \left(\hat{y}_{far,RI} - \hat{y}_{near,RI}\right)^2 + \left(\hat{z}_{far,RI} - \hat{z}_{near,RI}\right)^2}. \tag{3}$$

The IUT is considered to be in compliance with regard to range error if $\left|E_{range}\right| \leq \mathrm{MPE}_{range}$.

The RMS dispersion limit L_{RMS} is calculated as

$$L_{RMS} = \max_{RMS}\{\mathrm{RMS}_{near}, \mathrm{RMS}_{far}\}. \tag{4}$$

The IUT is considered to be in compliance with regard to RMS dispersion if $L_{RMS} \leq \mathrm{MPL}_{RMS}$.

If the IUT fails either of these compliance tests, then a single retest is permitted. If the IUT fails either of these compliance tests during the retest, then the IUT is deemed to be out-of-compliance with regard to the manufacturer-supplied specifications. If, however, the IUT passes the retest, then it is considered to be in compliance.

4   NRCC Experiments

The procedures described in the proposed standard were performed at the NRCC. The purpose of these experiments was to identify issues related to the test procedure and develop best practices to address these issues. A rectangular target plate was placed on a rail system to characterize the range error performance of a medium-range 3D imaging system. For this example, the identities of the RI and IUT have been obfuscated because this was not a formal evaluation of the IUT or the RI. The procedures described here can be applied to target plates mounted on either a rail or on stands.

4.1   Experimental Design

The layout of the experiment is illustrated in Figure 5 and consists of a rectangular target rigidly mounted on a plate, which is attached to a locking slider mounted on a rail system. Four SMR nests are mounted on the plate: two immediately below the rectangular target, and two immediately above the rectangular target. Figure 5(a) is a side view of the test system to illustrate the position of the RI relative to the target plate, and Figure 5(b) shows a front view that highlights the positions of the SMRs used by the RI. The position of the IUT, not shown in Figure 5, is such that the geometric center of the target plate remains, as much as possible, along a line through the origin of the IUT.
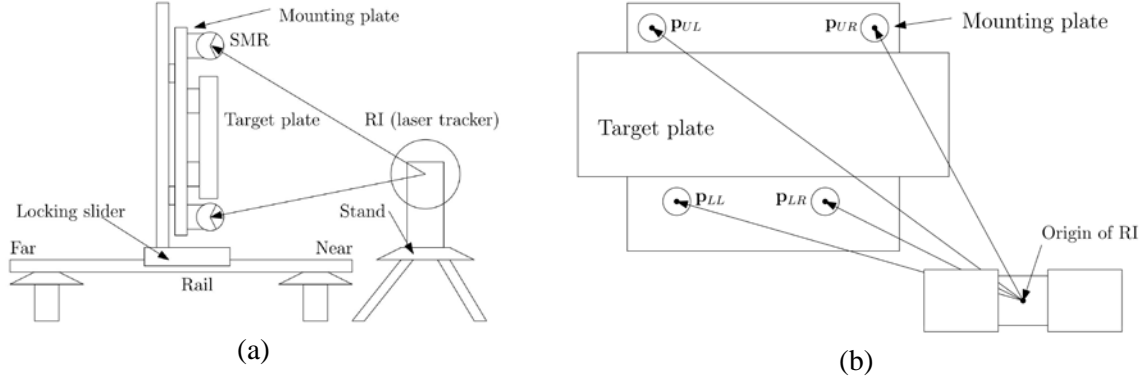
Figure 5: Test setup using a rail-mounted target plate. (a) Side view showing the position of the RI, target plate, and SMRs. (b) Front view showing the position of the RI, in front and to one side of the target plate, as well as the distribution of the SMRs.

4.2 Modelling the target assembly

The first step in the procedure employed by NRCC was to link a digital model of the target plate to the positions of the SMR mounts on the mounting plate, as shown on Figure 5. The purpose of this step is to generate a single model of the target plate that can be referenced no matter where the combination of target-plate and mounting-plate is moved. The RI actively tracks the locations of the SMRs in the mounting plate regardless of its position along Line A. This allows us to avoid having to remeasure the positions and orientations of the front and side planes of the target plate.

The assembly is placed in a position near the RI, then a 1.5 inch (38.1 mm) diameter SMR is used to perform three to five measurements of each of the four sides of the target and at least five measurements of the front of the target plate. For each of these five planar surfaces, measurements are performed at positions far from each other to ensure that the final model is a reasonable representation of each planar surface. Note that this measurement process only needs to be performed once to link the model of the target plate to the positions of the SMR mounts on the mounting plate.

A plane is fit to each of the five surfaces: $\mathbf{R}_{top}$ from the top plane and $\mathbf{R}_{bottom}$ from the bottom plane under the contraint that both planes be parallel to each other, $\mathbf{R}_{left}$ from the left plane and $\mathbf{R}_{right}$ from the right plane under the contraint that both planes be parallel to each other, and $\mathbf{R}_{front}$ from the front plane. A plane $\mathbf{R}_{vertical}$ is generated as the plane equidistant between $\mathbf{R}_{left}$ and $\mathbf{R}_{right}$, a plane $\mathbf{R}_{horizontal}$ is generated as the plane equidistant between $\mathbf{R}_{top}$ and $\mathbf{R}_{bottom}$, and the reference geometric center of the target-plate face $\boldsymbol{p}_{center}$ is then extracted as the intersection of $\mathbf{R}_{vertical}$, $\mathbf{R}_{horizontal}$, and $\mathbf{R}_{front}$. The positions of the SMRs on the mounting plate, denoted $\mathbf{p}_{UL}$, $\mathbf{p}_{UR}$, $\mathbf{p}_{LL}$, and $\mathbf{p}_{LR}$ in Figure 5(b), are then obtained relative to $\boldsymbol{p}_{center}$ so that the geometric center of the target plate can be extracted from the positions of the SMRs on the mounting plate, regardless of where the assembly is subsequently positioned.

4.3 Calculation of Distance

The assembly, shown in Figure 3(b), is placed in the near and far position on the rail. At each position, both the SMR positions and a scan of the target-plate surface are obtained. Given measurements at two positions on the rail, the reference distance, d_{RI}, between the two target-plate positions was found using (3).

Table 1: Results of six repetitions of the proposed range measurement error procedure. Each distance value is the difference between a single scan at the far position and a single scan at the near position. All results are given in millimeters.

Repetition	1	2	3	4	5	6	Average
d_{RI}	2035.00	2033.37	2030.89	2035.05	2034.90	2034.91	N/A
d_{IUT}	2034.72	2033.10	2030.65	2034.77	2034.65	2034.61	N/A
$\left|E_{range}\right|$	0.28	0.27	0.24	0.28	0.25	0.30	0.27 ±0.02
L_{RMS}	0.167	0.171	0.164	0.162	0.185	0.166	0.169±0.008

Immediately after performing RI measurements for any given position on the rail, the IUT was used to obtain a surface map of the target-plate face. Given measurements at the near and far positions, the geometric centers of the target-plate faces were obtained using the procedure described in Section 3.2.2. The IUT distance between target-plate geometric centers in the near and far positions was then found using (2). The RMS dispersion values RMS_{near} and RMS_{far} were also generated at this time.

4.4 Analysis of Results

Table 1 shows the results of six repetitions of the procedure described in the proposed standard. In practice, the procedure would only have been performed once with a second repetition performed only if the IUT was found not to be in compliance.

The first two rows are used to calculate E_{range} for the IUT with respect to the RI. The values in each column are the distance between the geometric center of the bounding box that encompasses all points associated with the target plate face acquired at the far position and the geometric center of the bounding box that encompasses all points associated with the target plate face acquired at the near position. The average absolute value of $\left|E_{range}\right|$ was (0.27 ± 0.02) mm, indicating that the results are repeatable. If the IUT were being evaluated as recommended in the proposed standard, then only the first repetition would have been used as the calculated absolute value of the range measurement error; that is, $\left|E_{range}\right| = 0.28$ mm. If the manufacturer's specified MPE for the IUT is $MPE_{range} = 0.30$ mm, then $\left(\left|E_{range}\right| = 0.28\right) \le \left(MPE_{range} = 0.30\right)$ so the IUT would be in compliance.

The last row shows the L_{RMS} for each repetition. The average RMS dispersion was (0.169 ± 0.008) mm, indicating that the results are repeatable. If the IUT were being evaluated as recommended in the proposed standard, then only the first repetition would have been used as the calculated RMS dispersion limit; that is $L_{RMS} = 0.167$ mm. If the manufacturer's specified MPL for the IUT is $MPL_{RMS} = 0.20$ mm, then $(L_{RMS} = 0.167) \le (MPL_{RMS} = 0.20)$ so the IUT is in compliance.

5 Conclusions

A Proposed Standard ASTM E57.02 "Test Method to Evaluate the Range Measurement Performance of 3D Imaging Systems in the Medium Range" is currently under development by the ASTM E57 committee. The proposed standard was submitted for ASTM E57.02 subcommittee ballot in February 2013. The purpose of the standard is to provide metrics and procedures to evaluate the range measurement performance of medium-range 3D imaging systems. We presented a summary of the document to date, the proposed test methods, the current status of the proposed standard, and results of experiments performed at the NRCC.

6 Acknowledgments

References

[1] Robson, S., Beraldin, A., Brownhill, A., MacDonald, L., *Artefacts for optical surface measurement,* Society of Photo-Optical Instrumentation & Electronics & Society for Imaging Science and Technology, in Videometrics, Range Imaging, and Applications XI (2011).

[2] Cheok, G.S., Lytle, A.M., Saidi, K.S., *ASTM E57 3D Imaging Systems Committee: An Update*, In: Laser Radar Technology and Applications XII – Proceedings of the SPIE, Vol. 6950, doi:10.1117/12.791929 (2008).

[3] Cheok, G.S., Saidi, K.S., Lytle, A.M., *Evaluating a Ranging Protocol for 3D Imaging Systems*, In: Proceedings of the 24th International Symposium on Automation & Robotics in Construction (2007).

[4] Cheok, G.S., Saidi, K.S., Franaszek, M., *Target-Penetration of Laser-Based 3D Imaging Systems*, In: Three-dimensional Imaging Metrology - Proceedings of the SPIE-IS&T Electronic Imaging, Vol. 7239, doi:10.1117/12.804929 (2009).

[5] Phillips, S., Krystek, M., Shakarji, C., Summerhays, K., *Dimensional measurement traceability of 3D imaging data*, In: Three-dimensional Imaging Metrology - Proceedings of the SPIE-IS&T Electronic Imaging, Vol. 7239, doi:10.1117/12.816498 (2009).

[6] Bridges, R., *Ways to verify performance of 3D imaging instruments*, In: Three-dimensional Imaging Metrology - Proceedings of the SPIE-IS&T Electronic Imaging, Vol. 7239, doi:10.1117/12.805987 (2009).

[7] Beraldin, J.-A., Cournoyer, L., Picard, M., Blais, F., *Proposed procedure for a distance protocol in support of ASTM-E57 standards activities on 3D imaging*, In: Three-dimensional Imaging Metrology - Proceedings of the SPIE-IS&T Electronic Imaging, Vol. 7239 doi:10.1117/12.814926 (2009).

[8] Beraldin, J.A., *Basic Theory on Surface Measurement Uncertainty of 3D Imaging Systems*, In: Three-Dimensional Imaging Metrology, Proceedings of the SPIE-IS&T Electronic Imaging, Vol. 7239, doi:10.1117/12.804700 (2008).

[9] ASTM E284-03a: *Standard Terminology for Appearance*, ASTM International, 2003.

[10] Cheok, G. S., Saidi, K. S., Franaszek, M., Filliben, J. J., and Scott, N. A., *Characterization of the Range Performance of a 3D Imaging System*, NIST TN 1695, Gaithersburg, MD (2011).

[11] Shakarji, C.M., *Least-Squares Fitting Algorithms of the NIST Algorithm Testing System*, Journal of Research of the National Institute of Standards and Technology, Vol. 103(6), (1998).